

High-Pressure Phase Equilibria of the Pseudoternary Mixture Sunflower Oil + Ethanol + Carbon Dioxide

Elvis J. Hernández,[†] Guillermo D. Mabe,[‡] Francisco J. Señoráns,[†] Guillermo Reglero,[†] and Tiziana Fornari^{*†}

Sección Departamental de Ciencias de la Alimentación, Universidad Autónoma de Madrid, Campus de Cantoblanco, 28049 Madrid, Spain, and Planta Piloto de Ingeniería Química, Camino La Carrindanga Km 7, 8000 Bahía Blanca, Argentina

Carbon dioxide can act as an expanding medium to carry out enzymatic reactions. Particularly, by dissolving CO₂ in mixtures comprising lipid-type substances and simultaneously increasing the pressure, the miscibility among reactants is enhanced, viscosity of the reaction mixture decreases, and diffusion of reactants and products is improved. Knowledge about the phase equilibrium behavior of the reactive mixture + CO₂ allows an adequate selection of conditions to achieve the homogeneous phase during reaction. In this work, phase equilibria data of the pseudoternary system sunflower oil + ethanol + CO₂ at two different conditions (313 K and 13 MPa; 333 K and 20 MPa) were investigated to provide an understanding of the phase behavior of vegetable oil ethanolysis reactions in CO₂-expanded media. Measurements were carried out by the analytical static method, using a variable-volume view cell equipped with a cold end light and a magnetic stirrer. Experimental tie-lines were determined for both types of equilibria observed: liquid + liquid and liquid + supercritical phase equilibria. Additionally, the experimental compositions obtained were correlated using a group contribution thermodynamic model.

Introduction

Catalytic reactions in supercritical or CO₂-expanded media are being intensely studied. Dense carbon dioxide as a reaction medium is expected to play an important role in environmentally benign processing.¹ One of these applications is the lipase-catalyzed ethanolysis of vegetable oils to produce monoglycerides and diglycerides.^{2,3} These substances have numerous applications in the food industry, such as emulsifiers for the preparation of processed foods, fat substitutes, and starting materials for the synthesis of defined lipids. Lipase-catalyzed reactions can selectively improve the production of one type of product or another (monoglycerides or diglycerides).

Lipase-catalyzed ethanolysis of vegetable oils in CO₂-expanded media preferably requires a single homogeneous liquid phase during reaction. Thus, knowledge of the phase equilibrium behavior of the reactive mixture with CO₂ allows the selection of adequate ethanolysis conditions, such as temperature, pressure, ethanol/oil ratio, and amount of CO₂ dissolved.

Binary experimental data related with high-pressure phase equilibria of mixtures comprising CO₂ and triglycerides, edible oils, or other lipid-type substances are extensively reported in the literature, and the reader is referred to the review presented by Güçlü-Üstündağ and Temelli.⁴ Additionally, high-pressure liquid–vapor data of the binary ethanol + CO₂ has also been widely investigated and reported (as an example, the work of Joung et al.⁵ is referred). With regard to the ternary CO₂ + ethanol + oil system rather the solubility of the oil in supercritical CO₂ with ethanol as a modifier was reported.⁶ Ndiaye et al.⁷ presented phase equilibrium data of binary and ternary systems involving CO₂, ethanol, soybean oil, castor oil, and their fatty acid ethyl esters in the temperature range of (286

to 343) K, pressures up to 27 MPa, and CO₂ overall composition ranging from (5 to 45) % w/w. Additionally, the work of Geana and Stainer⁸ presented two-phase equilibrium data (for the system rapeseed oil + ethanol + CO₂) in the temperature range of (313 to 353) K and at pressures of (6 to 12) MPa.

In this work, the phase equilibrium behavior of the pseudoternary sunflower oil + ethanol + CO₂ mixture was investigated at different conditions of temperature and pressure (313 K and 13 MPa; 333 K and 20 MPa). Phase equilibrium was experimentally studied employing the static method and a variable-volume cell. Liquid + supercritical phase equilibrium was observed when high a concentration of CO₂ was fed inside the cell, while liquid + liquid equilibrium was attained in the low CO₂ concentration range. In both cases, at a given temperature and pressure, samples of the phases in equilibrium were withdrawn from the equilibrium cell, and composition was determined to obtain the corresponding tie-lines.

The group contribution equation of state (GC-EoS) as developed by Skjold-Jørgensen⁹ was employed to correlate the experimental data obtained for both types of phase equilibria. This model has been previously applied to represent phase equilibria of CO₂ + lipid-type substances.¹⁰

Materials and Methods

Chemicals. Sunflower oil, with less than 0.5 % w/w of humidity, according to supplier specifications, was used in the present study. The sunflower oil fatty acid composition (w/w) was 7.5 % palmitic acid, 0.2 % palmitoleic acid, 14.7 % stearic acid, 43.6 % oleic acid, and 34 % linoleic acid. Ethanol absolute (water content < 0.1 % w/w) was obtained from Panreac (Barcelona, Spain) and was dried with molecular sieves 4 Å from Sigma-Aldrich (St. Louis, MO, USA). Carbon dioxide N38 (99.98 %) was purchased from AL Air Liquid España S. A. (Madrid, Spain).

Equipment and Experimental Procedure. Experimental measurements were carried out by a static method using a high-

* Corresponding author. Fax: +34-914978255. Phone: +34-914972380. E-mail: tiziana.fornari@uam.es.

[†] Universidad Autónoma de Madrid.

[‡] Planta Piloto de Ingeniería Química.

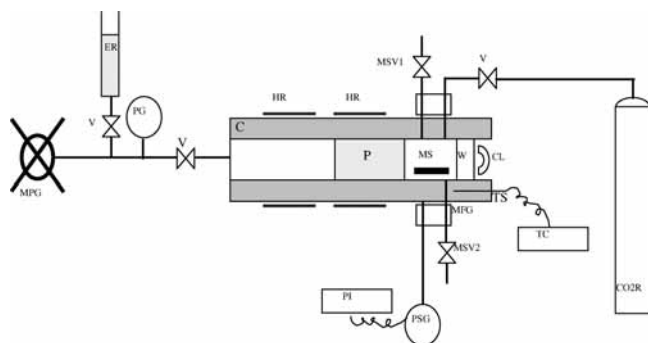


Figure 1. Experimental device employed to high-pressure phase equilibria measurements. C, variable-volume cell; P, piston; MPG, manual pressure generator; MS, magnetic stirrer; W, glass window; CL, cold light; HR, heating resistances; MFG, magnetic field generator; TS, temperature sensor; TC, temperature controller; PS, pressure sensor; PI, pressure indicator; ER, ethanol reservoir; CO₂R, CO₂ reservoir; V, on-off valve; MSV1 and MSV2, micrometering sampling valves; PG, pressure gauge.

pressure variable-volume cell (see Figure 1). The equipment consists of a variable-volume cell, supplied with a front window and cold end light to observe phase segregation. The cell has a maximum capacity of 120 cm³ and comprises a cylinder and a piston, both made of stainless steel with a mirror finish, to allow a smooth displacement of the piston inside the cylinder. The movable piston has a double seal (Polypak from Parker) to separate the equilibrium chamber from the pressurizing circuit. The piston is driven by a manual pressure generator (HIP model 62-6-10), and ethanol was utilized as the pressurizing fluid.

The cell has a front window for visual observation, and illumination is provided by a cold end light. Screw retainers are used to hold the glass windows with a pair of Viton O-rings for sealing. A Teflon-coated magnetic bar, driven by an external alternating magnetic field, provides appropriate stirring inside the cell.

The cylinder is surrounded by a 20 mm thick aluminum jacket, externally heated by two electrical resistances connected

to a temperature controller (Glas-Col). The temperature is measured by a 100 Ω Pt resistance thermometer, placed inside a groove in the aluminum jacket, and is controlled to within ± 0.1 K. A gauge transducer (Barksdale) coupled with a digital indicator (Redlion) is connected to one of the four capillary lines. The estimated accuracy of the pressure measurements is ± 0.02 MPa. The rest of the capillary lines are employed to feed chemicals and to sample.

Weighted amounts of ethanol and sunflower oil were introduced into the cell, which was purged with CO₂ to remove the residual air. Then, a weighted mass of CO₂ was let to flow into the cell. Once the temperature was stabilized, the desired pressure was achieved (by means of the manual pressure generator), and the magnetic stirrer was turned on. After 1.5 h, stirring was stopped, and the mixture was let to repose for 3 h in order that phase segregation occurred. The front window with the cold end light was employed for visual verification of the existence of one or two phases. The stirring and repose times were established according to preliminary experiments carried out in the liquid + supercritical phase equilibria region. The repose times applied in the case of liquid + liquid equilibria were longer (up to 5 h), in order that a definite and clear interface was kept inside the equilibrium cell for at least two hours.

Samples were withdrawn through capillary lines and micrometering valves and decompressed to atmospheric pressure. Both valves were thermostated at the same temperature of the equilibrium cell. The manual pressure generator was employed to keep pressure constant during sampling.

Ethanol and the oil were collected in glass vials and separated from the CO₂ by using a cool trap. Vials were weighed in a precision analytical balance and placed in a heater at 323 K where ethanol was eliminated by evaporation. Then, vials were weighted again to determine the amount of ethanol evaporated from the sample and the amount of remained material (sunflower oil).

Table 1. Liquid + Liquid (L + L) and Liquid + Supercritical (L + SC) Phase Compositions (% Weight) of the Pseudo-Ternary Mixture CO₂ (1) + Ethanol (2) + Sunflower Oil (3) at 313 K and 13 MPa

heavy phase			light phase			type of phase equilibria
w ₁	w ₂	w ₃	w ₁	w ₂	w ₃	
0.00 ± 0.00	15.26 ± 0.42	84.74 ± 0.42	0.00 ± 0.00	92.83 ± 0.37	7.17 ± 0.37	L + L
6.73 ± 0.53	18.68 ± 0.25	74.57 ± 0.78	13.83 ± 0.12	81.35 ± 0.71	4.82 ± 0.59	L + L
16.56 ± 0.31	20.96 ± 0.62	62.47 ± 0.31	26.89 ± 0.43	58.3 ± 0.12	14.80 ± 0.31	L + L
26.20 ± 0.61	0.00 ± 0.00	73.80 ± 0.61	100.00 ± 0.00	0.00 ± 0.00	0.00 ± 0.00	L + SC
31.00 ± 0.08	2.60 ± 0.11	66.40 ± 0.03	95.68 ± 0.21	4.32 ± 0.21	0.00 ± 0.00	L + SC
31.73 ± 0.54	6.92 ± 0.23	61.35 ± 0.77	90.17 ± 0.37	9.83 ± 0.37	0.00 ± 0.00	L + SC
31.96 ± 0.62	11.03 ± 0.12	57.01 ± 0.50	84.55 ± 0.85	14.95 ± 0.32	0.50 ± 0.53	L + SC
34.13 ± 0.37	16.14 ± 0.06	49.73 ± 0.43	58.45 ± 0.93	37.50 ± 0.76	4.05 ± 0.16	L + SC
31.47 ± 0.03	50.03 ± 0.38	18.50 ± 0.35	32.53 ± 0.22	49.01 ± 0.22	18.46 ± 0.44	homogeneous phase

Table 2. Liquid + Liquid (L + L) and Liquid + Supercritical (L + SC) Phase Compositions (% Weight) of the Pseudo-Ternary Mixture CO₂ (1) + Ethanol (2) + Sunflower Oil (3) at 333 K and 20 MPa

heavy phase			light phase			type of phase equilibria
w ₁	w ₂	w ₃	w ₁	w ₂	w ₃	
0.00 ± 0.00	23.05 ± 0.34	76.95 ± 0.34	0.00 ± 0.00	87.77 ± 0.55	12.23 ± 0.55	L + L
7.37 ± 0.21	24.84 ± 0.01	67.79 ± 0.20	9.03 ± 0.40	77.72 ± 0.07	13.25 ± 0.47	L + L
10.41 ± 0.53	25.28 ± 0.82	64.31 ± 0.29	13.08 ± 0.63	72.44 ± 0.31	14.48 ± 0.32	L + L
28.04 ± 0.36	0.00 ± 0.00	71.96 ± 0.36	100.00 ± 0.00	0.00 ± 0.00	0.00 ± 0.00	L + SC
31.74 ± 0.19	4.04 ± 0.11	64.18 ± 0.30	93.72 ± 0.10	6.28 ± 0.10	0.00 ± 0.00	L + SC
33.92 ± 0.23	8.47 ± 0.51	57.60 ± 0.74	89.11 ± 0.65	10.88 ± 0.65	0.01 ± 0.00	L + SC
36.45 ± 0.35	11.38 ± 0.45	52.17 ± 0.10	84.30 ± 0.56	15.69 ± 0.16	0.01 ± 0.72	L + SC
37.87 ± 0.57	14.02 ± 0.73	48.11 ± 0.16	77.21 ± 0.47	20.69 ± 0.23	2.09 ± 0.24	L + SC
41.11 ± 0.26	16.24 ± 0.56	42.65 ± 0.30	69.05 ± 0.07	24.66 ± 0.13	6.29 ± 0.06	L + SC
42.95 ± 0.37	30.54 ± 0.15	26.53 ± 0.22	43.01 ± 0.21	29.35 ± 0.46	27.64 ± 0.25	homogeneous phase
24.89 ± 0.14	28.86 ± 0.41	46.25 ± 0.27	25.04 ± 0.52	27.96 ± 0.31	47.00 ± 0.21	homogeneous phase
19.52 ± 0.27	25.67 ± 0.16	54.81 ± 0.11	18.96 ± 0.11	26.02 ± 0.11	55.02 ± 0.22	homogeneous phase

The amount of CO₂ was determined volumetrically using a 1000 mL graduated tube filled with a saturated solution of Na₂SO₄ to prevent CO₂ dissolution. The volume of gas was quantified as the displaced liquid volume and corrected by accounting for the effects of temperature, atmospheric pressure, and water vapor pressure.

All samples were collected by duplicate, even when a single homogeneous phase was observed inside the cell. Deviations between the resulted mass fractions were lower than 1 % in all measurements.

GC-EoS Model. The residual Helmholtz energy in the GC-EoS model⁹ is described by two terms

$$A^{\text{res}} = A^{\text{fv}} + A^{\text{att}} \quad (1)$$

The free volume contribution (A^{fv}) is modeled assuming hard sphere behavior for the molecules, characterizing each substance i by a hard sphere diameter d_i . A Carnahan–Starling type of hard sphere expression for mixtures is adopted

$$A^{\text{fv}}/RT = 3(\lambda_1\lambda_2/\lambda_3)(Y-1) + (\lambda_2^3/\lambda_3^2)(-Y+Y^2-\ln Y) + n \ln Y \quad (2)$$

where

$$Y = \left(1 - \frac{\pi\lambda_3}{6V}\right)^{-1} \text{ and } \lambda_k = \sum_i^{NC} n_i d_i^k$$

NC is the number of components; n_i is the number of moles of component i ; and V is the total volume. A temperature-dependent generalized expression is assumed for d_i

$$d_i = 1.065655d_{ci}\{1 - 0.12 \exp[-2T_{ci}/(3T)]\} \quad (3)$$

d_{ci} is the pure component critical hard sphere diameter, given by

$$d_{ci} = (0.08943RT_{ci}/P_{ci})^{1/3} \quad (4)$$

when the compound matches with a group (e.g., H₂O, CO₂, H₂, etc.). For the remaining cases, d_{ci} is fitted to a point of the pure component vapor pressure curve, usually the normal boiling point. Since vapor pressure data for low volatile or thermolabile substances are often not available or not reliable, infinite dilution activity coefficients can be used to estimate the d_{ci} parameter of high molecular weight compounds, such as alkanes and triglycerides, as demonstrated by Espinosa et al.¹³

For the evaluation of the attractive contribution to the Helmholtz energy, a group contribution version of a density-dependent NRTL-type expression is derived

$$A^{\text{att}}/RT = -\frac{z}{2} \sum_i^{NC} n_i \sum_j^{NG} v_j^i q_j \sum_k^{NG} (\theta_k g_{kj} \tilde{q} \rho) / \sum_l^{NG} \theta_l \tau_{lj} \quad (5)$$

where

$$\theta_j = (q_j/\tilde{q}) \sum_i^{NC} n_i v_j^i \quad (6)$$

$$\tilde{q} = \sum_i^{NC} n_i \sum_j^{NG} v_j^i q_j \quad (7)$$

$$\tau_{ij} = \exp[\alpha_{ij} \Delta g_{ij} \tilde{q} / (RTV)] \quad (8)$$

$$\Delta g_{ij} = g_{ij} - g_{ji} \quad (9)$$

NG is the number of groups; z is the number of nearest neighbors to any segment (set to 10); v_j^i is the number of groups type j in molecule i ; q_j is the number of surface segments

assigned to group j ; θ_k is the surface fraction of group k ; \tilde{q} is the total number of surface segments; g_{ij} is the attraction energy parameter for interactions between groups i and j ; and α_{ij} is the NRTL nonrandomness parameter ($\alpha_{ij} \neq \alpha_{ji}$). The interactions between unlike groups are calculated from

$$g_{ij} = k_{ij}(g_{ii}g_{jj})^{1/2} \quad (k_{ij} = k_{ji}) \quad (10)$$

with the following temperature dependences for the interaction parameters

$$g_{ij} = g_{ij}^* (1 + g'_{ij}(T/T_j^* - 1) + g''_{ij} \ln(T/T_j^*)) \quad (11)$$

$$k_{ij} = k_{ij}^* \{1 + k'_{ij} \ln[2T/(T_i^* + T_j^*)]\} \quad (12)$$

being g_{ij}^* the interaction parameter at the reference temperature T_i^* .

Results and Discussion

Tables 1 and 2 report the compositions obtained for the liquid + liquid (L + L) and liquid + supercritical (L + SC) tie-lines at the two different conditions of pressure and temperature investigated. The different two-phase regions observed are represented in Figure 2 (313 K and 13 MPa) and Figure 3 (333 K and 20 MPa). As can be observed in the figures, the compositions of the two liquid phases in equilibrium become more similar as the amount of CO₂ dissolved is increased. Similarly, the compositions achieved for the liquid and supercritical phases in the L + SC region become more similar as the amount of ethanol dissolved is increased. The existence of a homogeneous region (among the two-phase regions) was visually observed. Additionally, in the case of the homogeneous phase, samples were collected from the top and bottom of the equilibrium cell to determine their composition and verify that it was equal to the composition loaded in the equilibrium cell. As can be deduced from Figures 2 and 3, the homogeneous region is larger at 333 K and 20 MPa than at 313 K and 13 MPa.

The experimental phase equilibrium data obtained in this work have been represented using the GC-EoS. This model has two contributions to the residual Helmholtz energy of the system: a repulsive Carnahan–Starling free volume term and an attractive contribution term which is a group-contribution version of the NRTL model. The GC-EoS model

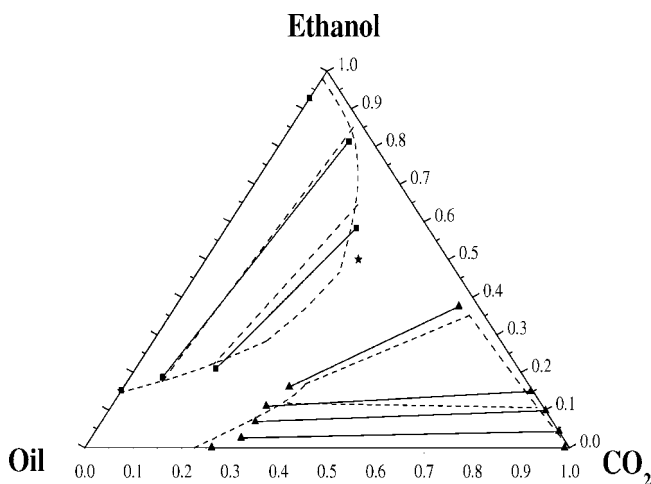


Figure 2. Phase diagram of the pseudoternary mixture sunflower oil + ethanol + CO₂ at 313 K and 13 MPa. ■, experimental L + L tie-line; ▲, experimental L + SC tie-line; ★, experimental homogeneous phase; - -, GC-EoS model.

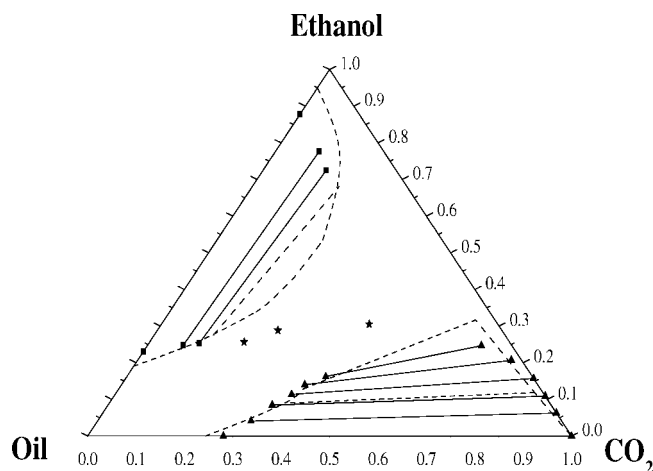


Figure 3. Phase diagram of the pseudoternary mixture sunflower oil + ethanol + CO₂ at 333 K and 20 MPa. ■, experimental L + L tie-line; ▲, experimental L + SC tie-line; ★, experimental homogeneous phase; ---, GC-EoS model.

Table 3. Pure Component Parameters

	T_c/K	p_c/MPa	$d_c/cm \cdot mol^{-1}$
CO ₂	304.2	7.28	3.125
ethanol	516.2	6.38	3.942
sunflower oil ^a	1044.0	0.45	12.19

^a T_c estimated using Fedors group contribution approach¹² and d_c value from Espinosa et al.¹³

Table 4. GC-EoS Pure Group and Binary Interaction Parameters Employed in This Work

Pure Group Parameters					
	reference temperature	surface area	pure group energy parameters ^a		
	T^*/K	q	g	g'	g''
CH ₃	600	0.848	316910.0	-0.9274	0.0
CH ₂	600	0.540	356080.0	-0.8755	0.0
CH=CH	600	0.867	403590.0	-0.7631	0.0
CH ₂ OH	512.6	1.124	1207500.0	0.644	0.0
(CH ₃ COO) ₂ CH ₂ COO triglyceride group (TG)	600	3.948	346350.0	-1.3460	0.0
CO ₂	304.2	1.261	531890.0	-0.5780	0.0
Binary Group Interaction Parameters					
i	j	attractive energy parameters		nonrandomness parameters	
		k_{ij}	k'_{ij}	α_{ij}	α_{ji}
CO ₂	CH ₃	0.898	0.0	4.683	4.683
	CH ₂	0.874	0.0	4.683	4.683
	CH=CH	0.948	0.0	0.0	0.0
	CH ₂ OH	1.115	0.094	-1.615	-1.615
	TG	1.094	0.112	-1.651	-1.651
TG	CH ₃ /CH ₂	0.860	0.0	0.0	0.0
	CH=CH	0.883	0.0	0.0	0.0
	CH ₂ OH ^b	1.912	0.151	15.00	10.90
	CH ₂ OH ^c	1.452	0.0	-12.10	-1.39
CH ₂ OH	CH ₃	0.715	0.0	10.22	1.471
	CH ₂	0.682	0.0	10.22	1.471
	CH=CH	1.006	0.0	-0.876	-0.876

^a $cm^6 \cdot atm \cdot mol \cdot (surface\ area\ segment)^{-2}$. ^b Parameters adjusted in this work using the L + L phase equilibrium data of Tables 1 and 2. ^c Parameters adjusted in this work using the L + SC phase equilibrium data of Tables 1 and 2.

equations are given in the Appendix, clearing up the required parameters to carry out phase equilibria calculations: pure group and binary group interaction parameters, together with

pure component parameters (critical temperature, critical pressure, and critical hard sphere diameter). For a detailed description of the model equations and parameters, the reader is referred to Skjold-Jørgensen.⁹

Pure-component parameters employed in this work for CO₂, ethanol, and sunflower oil are given in Table 3. Sunflower oil was represented as a pseudotriglyceride with the same molecular weight and number of unsaturated bonds as the real oil, as described by Fornari.¹¹ Taking into account the fatty acid composition of sunflower oil, the group composition of the pseudotriglyceride representing sunflower oil resulted to be: 1CH₃COO)₂CH₂COO (triglyceride group), 3CH₃, 42CH₂, and 3CH=CH (paraffin and olefin groups).

Pure group and binary group interaction parameters were obtained from the literature,¹⁰ except for the binary interaction parameters between the triglyceride group (TG) and the alcohol CH₂OH group which were not available in the literature and thus were fitted in this work using the present L + SC and L + L data. Table 4 gives all pure group and binary interaction parameters employed in this work, together with the TG-CH₂OH interaction parameters adjusted.

Figures 2 and 3 shows a comparison between the experimental data obtained and the phase equilibria representation achieved with the GC-EoS model using the parameters given in Table 4. A satisfactory representation of phase compositions and tie-line slopes was obtained. The main drawback of the thermodynamic modeling is that the oil content in the ethanolic phase of the binary ethanol + sunflower oil is rather underestimated. The average absolute relative deviations (AARD) between experimental and calculated tie-line compositions

$$AARD = \frac{1}{N_{exp}} \sum \left| \frac{z_i^{exp} - z_i^{cal}}{z_i^{exp}} \right|$$

are 20.41 %, 9.84 %, and 10.14 % for, respectively, CO₂, ethanol, and sunflower oil in the liquid (heavy) phase of the L + SC phase equilibria and 3.44 %, 18.01 %, and 30.62 % in the corresponding light phase. As can be deduced, the largest AARD values are related with the sunflower oil composition in the supercritical phase due to the low solubility of the oil in this phase. With respect to the L + L phase equilibria, the corresponding AARD values are 10.15 %, 13.77 %, and 4.09 % for, respectively, CO₂, ethanol, and sunflower oil in the heavy phase and 18.03 %, 7.36 %, and 45.90 % in the light phase. Again, major errors are produced in the calculation of the oil mole fraction in the ethanolic (light) phase.

The global AARD values obtained in the calculation of CO₂, ethanol, and sunflower oil mole fractions are, respectively, 12.65 %, 12.06 %, and 20.67 %.

With respect to the parameter regression procedure, it has to be pointed out that phase equilibria data corresponding to a ternary system (CO₂ + ethanol + sunflower oil) were employed to fit a binary (TG-CH₂OH) interaction. Thus, the TG-CH₂OH parameters resulting from the fitting procedure should be considered as an approach to evaluate the capability of the GC-EoS model to represent the high-pressure phase behavior of the triglyceride + ethanol + CO₂ ternary systems. As can be observed in Table 4, different TG-CH₂OH interaction parameters were necessary to correlate both types (L + L and L + SC) of phase equilibria. A more extensive set of binary ethanol + oil data would be necessary to study this deficiency of the model parameter table.

Conclusions

High-pressure phase equilibria data of the sunflower oil + ethanol + CO₂ mixture were experimentally obtained. Tie-lines of the pseudoternary diagram were determined, indicating the existence of two different liquid + liquid and liquid + supercritical phase regions. The homogeneous region was verified by visual observation and by sampling from the bottom and top of the equilibrium cell. This single-phase region would provide improved conditions to carry out the enzymatic ethanolysis of the oil when compared with the two-phase regions.

The experimental data obtained were correlated using the GC-EoS. The model was capable of representing both types of phase equilibria, but a different set of binary interaction parameters between the triglyceride and CH₂OH groups were required. The application of the GC-EoS model in a nearly predictive manner (almost all binary interaction parameters were obtained from the literature) brought to light some deficiencies of the model parameter table to represent phase equilibria of oil + ethanol + CO₂ mixtures.

Acknowledgment

This work has been financed by Universidad Autónoma de Madrid and Comunidad Autónoma de Madrid (projects CCG06-UAM/AGR-0075 and ALIBIRD S-505/AGR-0153). T. F. would like to acknowledge the financial support of the Ramon y Cajal Program from the Ministry of Education and Science.

Literature Cited

- (1) Subramaniam, B.; Lyon, C. J.; Arunajatesan, V. Environmentally benign multiphase catalysis with dense phase carbon dioxide. *Appl. Catal. B: Environ.* **2002**, *37*, 279–292.

- (2) Oliveira, D.; Oliveira, J. V. Enzymatic alcoholysis of palm kernel oil in *n*-hexane and SCCO₂. *J. Supercrit. Fluids* **2001**, *19*, 141–148.
- (3) Fornari, T.; Hernández, E. J.; Mabe, G. D.; Reglero, G.; Señoráns, F. J. Ethanolysis of sunflower oil in dense CO₂ catalyzed by *Pseudomonas cepacia* lipase. *Eur. J. Lipid Sci. Tech.*, submitted.
- (4) Güçlü-Üstündağ, O.; Temelli, F. Solubility behavior of ternary systems of lipids, cosolvents and supercritical carbon dioxide and processing aspects. *J. Supercrit. Fluids* **2005**, *36*, 1–15.
- (5) Joung, N. S.; Yoo, C. W.; Shin, H. Y.; Kim, S. Y.; Yoo, P.-K.; Lee, C. S.; Huh, W. S. Measurements and correlation of high-pressure VLE of binary CO₂–alcohol systems (methanol, ethanol, 2-methoxyethanol and 2-ethoxyethanol). *Fluid Phase Equilib.* **2001**, *185*, 219–230.
- (6) Güçlü-Üstündağ, O.; Temelli, T. Solubility behavior of ternary systems of lipids in supercritical carbon dioxide. *J. Supercrit. Fluids* **2006**, *38*, 275–288.
- (7) Ndiaye, P. M.; Franceschi, E.; Oliveira, D.; Dariva, C.; Tavares, F. W.; Oliveira, J. V. Phase behavior of soybean oil, castor oil and their fatty acid ethyl esters in carbon dioxide at high pressures. *J. Supercrit. Fluids* **2006**, *37*, 29–37.
- (8) Geana, D.; Seiner, R. Calculation of Phase Equilibrium in Supercritical Extraction of C54 Triglyceride (Rapeseed Oil). *J. Supercrit. Fluids* **1995**, *8*, 1071–18.
- (9) Skjold-Jørgensen, S. Gas Solubility Calculations. II. Application of a New Group-Contribution Equation of State. *Fluid Phase Equilib.* **1984**, *16*, 317–351.
- (10) Fornari, T. Revision and summary of the group contribution equation of state parameter table: application to edible oil constituents. *Fluid Phase Equilib.* **2007**, *262*, 187–209.
- (11) Fornari, T. Equilibrio Líquido-Vapor en Mezclas de Aceites Vegetales y Solventes, PhD Thesis, Univ. Nacional del Sur - Argentina, 1995.
- (12) Reid, R.; Prausnitz, J. M.; Poling, B. *The Properties of Gases and Liquids*, 4th ed.; Mc Graw-Hill Book Company: New York, 1987.
- (13) Espinosa, S.; Fornari, T.; Bottini, S. B.; Brignole, E. A. Phase equilibria in mixtures of fatty oils and derivatives with near critical fluids using the GC-EoS. *J. Supercrit. Fluids* **2002**, *23*, 91–102.

Received for review July 7, 2008. Accepted September 5, 2008.

JE800523J